

Upgrades to the ISS Water Recovery System

Matthew J. Kayatin,¹ Donald L. Carter,² Richard G. Schunk,³ and Jennifer M. Pruitt⁴
NASA George C. Marshall Space Flight Center, Huntsville, Alabama 35812, USA

The International Space Station Water Recovery System (WRS) is comprised of the Water Processor Assembly (WPA) and the Urine Processor Assembly (UPA). The WRS produces potable water from a combination of crew urine (first processed through the UPA), crew latent, and Sabatier product water. Though the WRS has performed well since operations began in November 2008, several modifications have been identified to improve the overall system performance. These modifications can reduce resupply and improve overall system reliability, which is beneficial for the ongoing ISS mission as well as for future NASA manned missions. The following paper details efforts to reduce the resupply mass of the WPA Multifiltration Bed, develop improved catalyst for the WPA Catalytic Reactor, evaluate optimum operation of UPA through parametric testing, and improve reliability of the UPA fluids pump and Distillation Assembly.

Nomenclature

<i>ARFTA</i>	=	advanced recycle filter tank assembly
$^{\circ}\text{C}$	=	degrees Celsius
<i>CCAA</i>	=	common cabin air assembly
<i>cm</i>	=	centimeter
<i>CWO</i>	=	catalytic wet oxidation
<i>d</i>	=	bed internal diameter
<i>DA</i>	=	distillation assembly
<i>DMSD</i>	=	dimethylsilanediol
<i>FCPA</i>	=	fluids control and pump assembly
<i>h</i>	=	hour
<i>ISS</i>	=	international space station
<i>L</i>	=	liter
<i>lb_m</i>	=	pound, mass
μ	=	micro
<i>MSFC</i>	=	marshall space flight center
<i>MTBF</i>	=	mean time between failures
<i>MF</i>	=	multifiltration
<i>mg</i>	=	milligram
<i>mhos</i>	=	conductivity, siemens
η	=	single pass adsorption efficiency
<i>OGS</i>	=	oxygen generation system
<i>ORU</i>	=	orbital replacement unit
<i>ppm</i>	=	parts per million, mass basis
<i>PCPA</i>	=	pressure control and pump assembly
<i>R&R</i>	=	remove and replace operation
<i>TIC</i>	=	total inorganic carbon
<i>TOC</i>	=	total organic carbon

¹ Aerospace Engineer, ECLS Systems, Space Systems Dept., NASA Marshall Space Flight Center/ES62

² ISS Water Subsystem Manager, ECLS Systems, Space Systems Dept., NASA Marshall Space Flight Center/ES62

³ Team Lead, Thermal Analysis and Control Branch, NASA Marshall Space Flight Center/EV34

⁴ ISS UPA Design Lead, ECLS Systems, Space Systems Dept., NASA Marshall Space Flight Center/ES62

<i>TOCA</i>	=	total organic carbon analyzer, located on ISS
<i>UPA</i>	=	urine processor assembly
<i>UTAS</i>	=	United Technology Aerospace Systems
<i>VCD</i>	=	vapor compression distillation
<i>VOC</i>	=	volatile organic compounds
<i>WRS</i>	=	water recovery system
<i>WPA</i>	=	water processor assembly

I. Introduction

The International Space Station (ISS) Water Recovery and Management System provides potable water for crew drinking and hygiene activities, oxygen generation, urinal flush water, and various payloads. To this end, wastewater is collected in the form of crew urine, humidity condensate, and Sabatier product water, and subsequently processed by the Water Recovery System (WRS) to potable water quality standards. This product water is provided to the potable bus for the various users, and is stored in water bags for future use when the potable bus needs supplementing. The WRS is comprised of the Urine Processor Assembly (UPA) and Water Processor Assembly (WPA), which are located in two International Standard Payload Racks named WRS-1 and WRS-2 as shown by Figure 1. This hardware was delivered to ISS on STS-126 on November 14, 2008 and initially installed in the US Lab module. On February 18, 2010, the racks were transferred to their permanent home in the Node 3 module. The layout of the two WRS racks is as shown in Fig. 1, along with the Oxygen Generation System (OGS). The WPA is packaged in WRS Rack 1 and partially in WRS Rack 2, linked by process water lines running between the two racks. The remaining portion of WRS Rack 2 houses the UPA. Detailed process descriptions and schematics of the entire WRS are provided by Pruitt et al. (2015)¹ and by Carter et. al (2015)². In addition, Ref. 1 provides detailed information regarding recent ISS WRS upgrade efforts.

A notable change to WRS-2 was made in 2016 to improve accessibility and urine brine transfer operations to and from the Advanced Recycle Filter Tank Assembly (ARFTA). A new door was installed on WRS-2 that includes a three-way valve to fill, drain, or process the installed ARFTA tank without having to remove it from the rack.

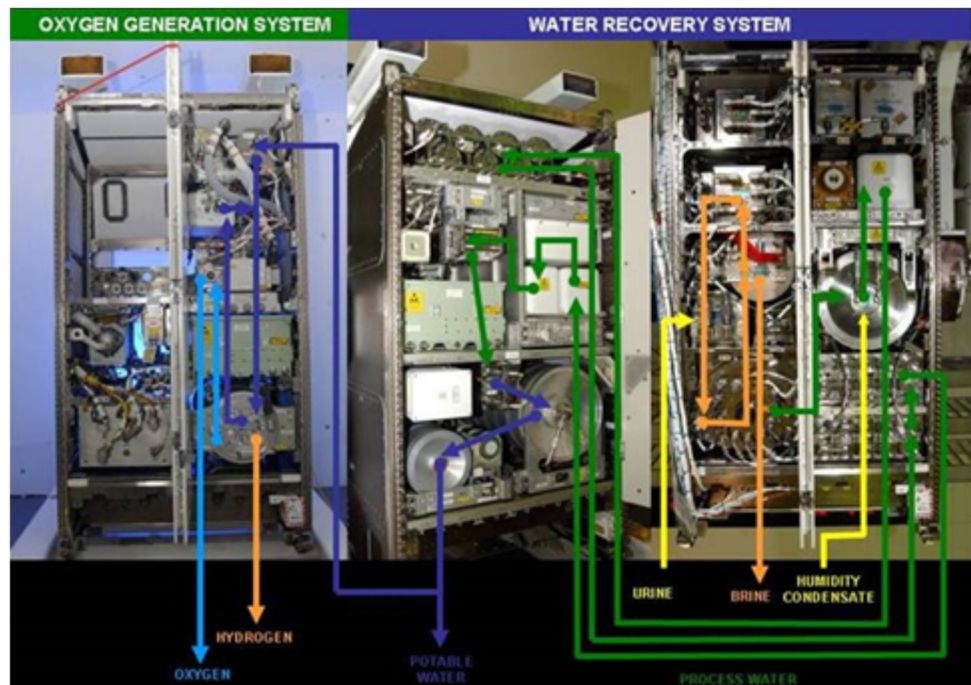


Figure 1. International Space Station Regenerative ECLSS Racks and process flows for the OGS and WRS.

II. Multifiltration Bed Lifetime Extension Testing

The WPA Multifiltration (MF) Beds comprise a significant resupply mass as required to support system operation. This resupply penalty is currently augmented because of the emergence of dimethylsilanediol (DMSD) in the WPA wastewater stream which necessitates replacement of both MF Beds more frequently than their nominal design lifetime.^{2,3} Ultimately, DMSD saturates the entire WPA system, is incompletely oxidized by the catalytic reactor, and therefore degrades the product water purity as indicated by the ISS Total Organic Carbon Analyzer (TOCA). There is an ongoing design effort to address DMSD by removing it from the cabin air stream entering the ISS Common Cabin Air Assembly (CCAA) and thus preventing contamination of the condensing heat exchanger located within.⁴ Node 1 air scrubbers were installed in ISS on May 12, 2015 and demonstrated that activated charcoal (Cabot GCA48) was capable of reducing detectable airborne siloxane levels; the influence on product water quality remains to be seen. Assuming that an engineering solution to controlling DMSD contamination will be successfully implemented,⁵ the lifetime of the MF Beds can theoretically be extended by employing a change in their operational approach and frequency of R&R, as described within.

The MF Beds utilize adsorption and ion exchange media to remove the majority of dissolved contaminants from the WPA wastewater stream. Ideally, once the 1st MF Bed is expended (as indicated by conductivity breakthrough), the 2nd MF Bed is moved into the 1st position and a fresh MF Bed is placed in the now vacant 2nd location. As designed, the MF beds are layered to specifically ensure ionic breakthrough occurs before non-volatile organic chemical breakthrough. Operating in this manner, only volatile organic compounds (VOC) pass through to the downstream catalytic reactor where they are ideally oxidized to primarily acetate and/or bicarbonate. Recognizing that these reactor products are identical to species the MF Beds remove, and comprise a substantial portion of the wastewater ionic load, it follows that allowing these species to break through the MF Beds and enter the catalytic reactor may extend MF Bed life and therefore reduce upmass. Initial testing at MSFC with a full-scale development catalytic reactor, Item 9503 of the Development Water Processor Package, P/N SVSK118440-1, demonstrated that typical bicarbonate and acetate levels in a saturated MF Bed effluent were within the reactor's oxidation capacity for a process Ersatz feed.⁷ Ultimately, the careful characterization of the MF Bed breakthrough products (sequence of breakthrough species, process conductivity) is required to determine both the viability and operational approach for allowing bicarbonate, acetate, and potentially ammonium to saturate one or both MF Beds prior to bed replacement.

To this end, ground testing at MSFC was conducted with two, in series, one-half scale flight MF Beds having a modified sorbent media layering design. The beds were challenged with 17,771 lb_m of total Ersatz water throughput and simultaneously monitored with process effluent conductivity sensors. Additional water sampling was done to characterize process pH, total organic carbon (TOC), total inorganic carbon (TIC), off-line conductivity, and ion chromatography (cations & anions) throughout the test duration for both bed effluent streams. The Ersatz water formulation was developed under ISS Program Office CR013322 and described by Rector et al. (2014).⁶ This formulation includes 22 mg/L of DMSD and testing at MSFC included the methanol hydrolysis byproduct (15.3 mg/L) from the dimethoxydimethylsilane precursor. All Ersatz water process tanks were quality controlled by the MSFC ES62 Chemistry Laboratory to verify matching ($\pm 10\%$) the theoretical TOC target of ≈ 56 ppm and the conductivity target of 170 $\mu\text{mho/cm}$. In order to facilitate acetate breakthrough, the flight layering was modified to remove Amberlite® IRN-77 and Amberlite® IRN-67. Additionally, Ambersorb® 4652 replaced the obsolete Barnebey-Cheney 580-26 activated charcoal layer. Table 1 displays the resin volumes loading into each one-half scale bed at MSFC.

Table 1. MF bed media type, volume, and orientation required for a single, one-half scale developmental MF bed. [†]Based on 580-26 bed volume.

Media Type	Bulk Density [g/L]	Volume [in ³]	Volume [cm ³]	Flow Orientation
Amberlite® IRN-150	690	462	7,570.8	TOP / OUTLET ↑ BOTTOM / INLET
Ambersorb® 4652	400	252 [†]	4,129.5	
	<i>SUM</i>	714	11,700	

Resin layers were separated by floating PTFE pucks with fine mesh retaining screens to allow for bed expansion or contraction during the test duration. Each half-scale bed was comprised of an aggregate of three media canisters of 3.3125 inch diameter.² The flight water flowrate of 13 lb_m/h was adjusted up to 15.6 lb_m/h to preserve superficial velocity in the half-scale beds in accordance with Eq. 1.

$$\frac{d_{Half-scale}^2}{d_{Flight}^2} = 1.21 \quad (1)$$

A. Process Conductivity Trends

Based on the 5 pairs of MF Beds used on ISS, the first flight MF Bed experiences initial breakthrough (presumably due to bicarbonate) of 10 $\mu\text{mhos/cm}$ after an average of approximately 3,200 L of throughput (see Appendix, Figure A1). The actual throughput to achieve breakthrough of acetate and ammonium is unknown because MF Bed replacement has always occurred prior to these events. Based on an average mass of Ersatz throughput of 125 lb_m per test day (56.7 L/day), it was anticipated that initial breakthrough would occur after approximately 28 test days for the first half-scale developmental aggregate MF Bed. As shown by Fig. 2, the initial onset of process conductivity rise was observed on day 56 after 6,897 lb_m (3,128 L) of Ersatz water throughput. Remarkably, when considering scale, this was approximately twice as long as compared to the flight beds (i.e. nearly equivalent volume throughput) at less than one half the total ion exchange resin volume. Recall that the media layering on orbit differs from the half-scale test bed. The full-scale ISS MF Beds each contain a total of 924 in^3 of IRN-150 plus additional volumes of ion exchange resins (IRN77 & IRA67). The half-scale developmental beds contain only IRN-150 and were packed with one half the in-flight volume (462 in^3). This result suggests that either the ion exchange capacities are significantly varied between flight and ground test beds (unlikely for such a large discrepancy of < 50%) or the ersatz formulation does not fully characterize the ionic load in ISS wastewater. ISS wastewater samples (US) showed TIC levels ($\mu \pm \sigma$) on the order of $21.5 \pm 9.7 \text{ mg/L}$ with a mean pH of 7.1. The bicarbonate level in the test Ersatz water was consistent with this load at 23.15 mg/L. Examining all TIC sources in the wastewater further we find little experimental evidence of elevated, unaccounted TIC. Due to the low pH of pretreated urine and process conditions in the distillation assembly (32 mm Hg; 85°F) it was expected that dissolved CO_2 would be degassed from solution. Indeed, ground testing of urine distillate showed a TIC level on the order of 5 mg/L at pH ~3.4. In addition, analyzed humidity condensate samples (US) returned from flight contained TIC levels ($\mu \pm \sigma$) of $33.8 \pm 13.8 \text{ mg/L}$ with a mean pH of 7.3. This is also consistent with the Ersatz load. However, recent theoretical predictions of pH dependent humidity condensate loading by Perry and Kayatin (2016) indicate inconsistencies between expected and measured grab sample TIC levels.⁸ Considering the ISS partial pressure of 3.5 mm Hg CO_2 (~ 8,000 mg/m^3) much more TIC is predicted than observed by grab sample analysis. In fact, at an average pH of 7.3 the condensate, the TIC load for 8,000 mg/m^3 cabin CO_2 is predicted to be on the order of 70 – 75 mg/L (see Fig. 7b in Ref. 8). This discrepancy may be due to both the differences in CO_2 solubility in the cold condensate (4.4°C) as well as losses occurring from the sampling, storage environment (ambient temp.), and sample transit (e.g. permeation effects). Given the apparent inherent inaccuracy associated with analysis of TIC (which includes dissolved carbon dioxide, bicarbonate, and carbonate), it is credible that significantly more bicarbonate is present in the ISS wastewater, resulting in earlier breakthrough on ISS.

Figure 2 displays the test stand in-line process conductivity sensor data for both half-scale MF Beds. All process conductivity data shown are representative of the daily final 100 lb_m tank averages. The inlet conductivity was remarkably consistent over the test lifetime averaging $173.7 \pm 3.8 \mu\text{mhos/cm}$. Highlighted are test days showing onset of ion breakthrough, the corresponding conductivity, and the cumulative mass throughput the system at that time. Bed #1 exhibited two conductivity plateaus each having an average magnitude of 10.51 $\mu\text{mhos/cm}$ (6 test day duration) and 35.58 $\mu\text{mhos/cm}$ (6 test day duration), respectively. Bed #2 exhibited two conductivity plateaus each having an average magnitude of 9.46 $\mu\text{mhos/cm}$ (3 test day duration) and 27.31 $\mu\text{mhos/cm}$ (20 test day duration), respectively. Scatter in the beginning of the 2nd plateau (~30 $\mu\text{mhos/cm}$) for Bed #2 were believed to be from the intermittent test stand operation over this time.

Flight process conductivity trends and water throughput are shown in Appendix A. The duration of the 1st conductivity plateau was on the order of 1,500 L (~ 3,315 lb_m) for MF Bed S/N 00009 starting with the 03/13 onset in conductivity rise. This plateau was not allowed to extend to complete breakthrough before flight bed change out, however, so this should be considered a lower approximate limit for its true duration. The duration of the first conductivity plateau for the half-scale Bed #1 (Fig. 2) was approximately 1,130 lb_m (510 L). This onset appears less sharp or of longer duration (3-4 test days) than the flight MF Bed data but analysis shows they are similar in length based on volume of water throughput. Comparing the duration of the flight and ground test beds, it appears that the length of the ground test bed duration is of reasonable magnitude. Unfortunately, since the true duration of the flight plateau is unknown, the conclusions that can be drawn by comparison are limited. As discussed in subsequent sections, the length of the ground test bed plateau would ultimately be determined by the Ersatz water formulation closely matching acetate ion loads with flight loads.

Note that influent to Bed #2 is subject to the breakthrough history of Bed #1 and thus the profiles of the two beds do not match (Fig. 2). It was anticipated that Bed #2's cumulative capacity for the breakthrough products of Bed #1 would be reduced and reflected in the conductivity profile. Indeed, the capacity for TIC was reduced as shown by the short 1st plateau. Conversely, the 2nd conductivity plateau for Bed #2 was much longer. As shown in subsequent

sections, the ion profile during this plateau does not exactly match Bed #1, and this must be taken in to consideration when interpreting results. It is noteworthy that the off-line, lab analyzed sample conductivity data for both developmental MF beds matched the in-line process conductivity sensor data trends well. Also, the 1st conductivity plateau of Bed #2 was so short that only one sample was captured for lab analysis resulting from the weekly (every 5 test days) sampling schedule.

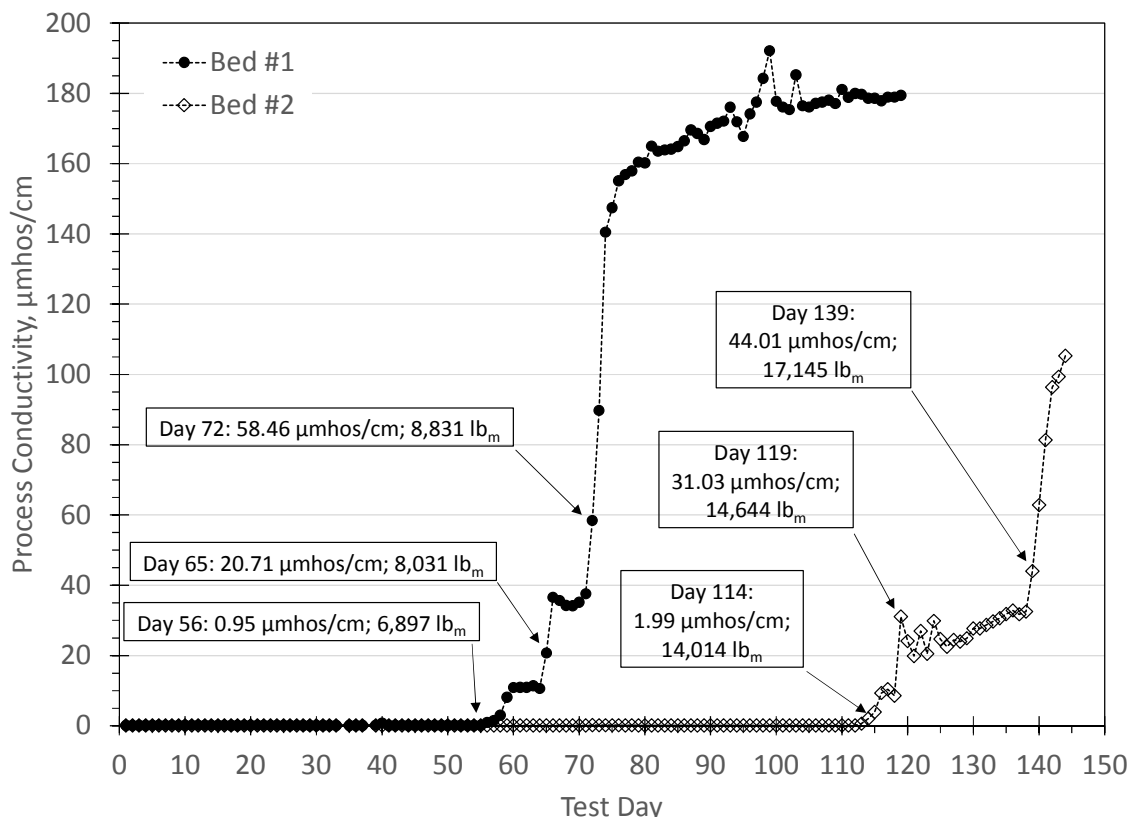


Figure 2. MF test stand in-line process conductivity sensor data for both half-scale MF Beds. Conductivities and mass cumulative Ersatz water throughput are shown at the onset of each breakthrough event. Average total daily mass throughput was 125 lb_m of Ersatz water.

B. Bed #1 Effluent Characterization

Figure 3 overlays the Bed #1 conductivity, major ion species, and pH correlations throughout breakthrough for the first 100 test days. The bed breakthrough profile was accompanied by a decrease in process pH over the 1st and 2nd conductivity plateaus before increasing upon complete ion breakthrough. Analysis of the major ionic constituents indicated the initial pH drop was first due to the breakthrough of dissolved TIC (pH dependent equilibrium of bicarbonate and carbonic acid)⁸, followed next by acetate (acetic acid). These two ions emerge as the main constituents in the 1st and 2nd conductivity plateaus. The onset of the final conductivity breakthrough was due to the additional breakthrough of the ammonium ion which also was accompanied by an increase the process pH. Potassium was the last major constituent to emerge over this period. It appears after complete ion breakthrough the effluent stream pH remained steady at approximately 7.7.

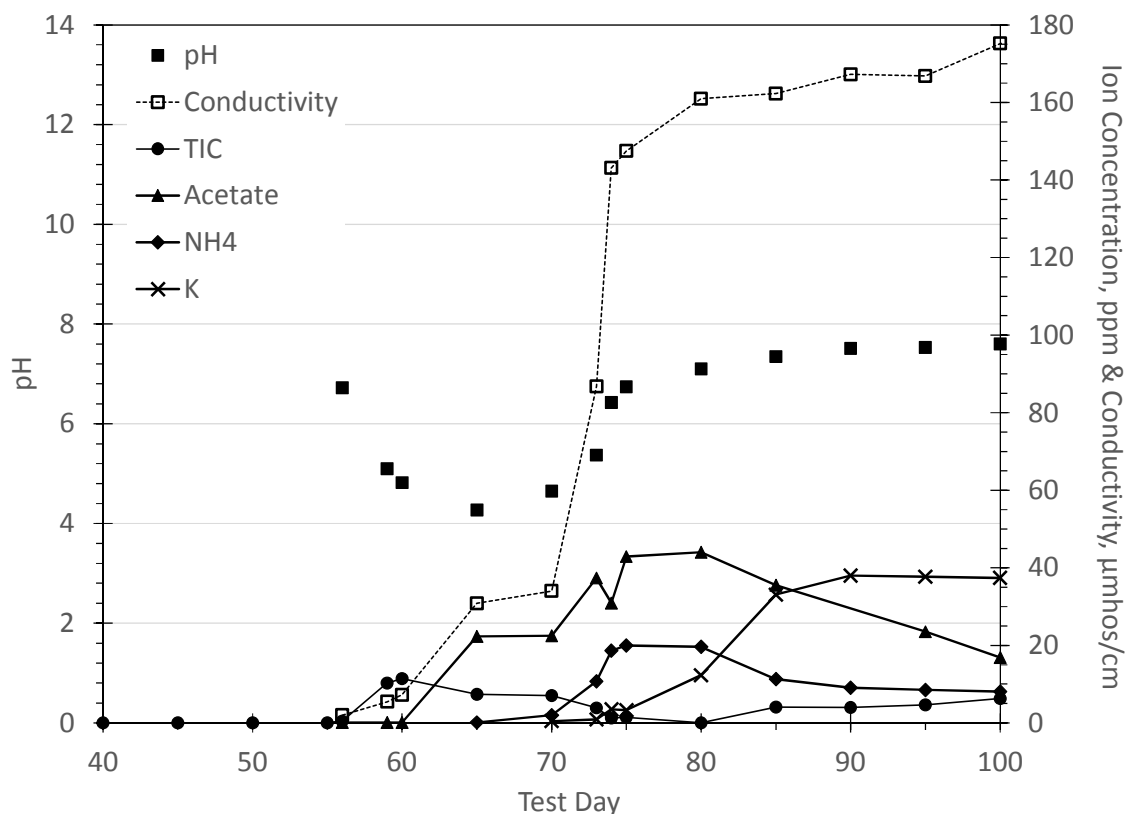


Figure 3. Bed #1 breakthrough conductivity, major ion species, and pH correlations for first 100 test days. All data are representative of aliquots sampled on the test day indicated and analyzed off-line by the MSFC ECLSS Chemistry Lab.

Figure 4 displays the complete Bed #1 breakthrough ion species profile. By stacking the cumulative ion data for each test day, ion breakthrough waves were observed. Overshooting waves were observed for TIC, acetate, ammonium, and to a lesser extent, calcium, sodium, and fluoride, indicating that these species were likely pushed off the bed by more strongly associating ions. Samples on Test Days 59 and 60 were taken within the 1st conductivity plateau and confirm the first species to break through was TIC. The next ion to breakthrough was acetate and, combined with the inorganic carbon, appeared to comprise the majority of the 2nd conductivity plateau shown on Test Day 65. Near the onset of the 3rd and final conductivity breakthrough rise (Day 70), sodium and ammonium appear at levels of 0.78 ppm and 2 ppm, respectively. Calcium, potassium, chlorine, and fluorine were detected at levels ≤ 0.5 ppm (Day 70). The plot shows that the largest contributor to the 3rd and final conductivity plateau were chloride, potassium, and ammonium. Although subjective, the general trend in appearance of ion breakthrough can be summarized as: TIC > acetate > ammonium > sodium \approx fluoride \approx calcium > potassium > chloride. Iodide (0.198 mg/L) was not analyzed in the test effluent. Due to its ion radius, it was assumed that iodide may be irreversibly adsorbed, or below detection, while exchanging within the current Ersatz formulation.

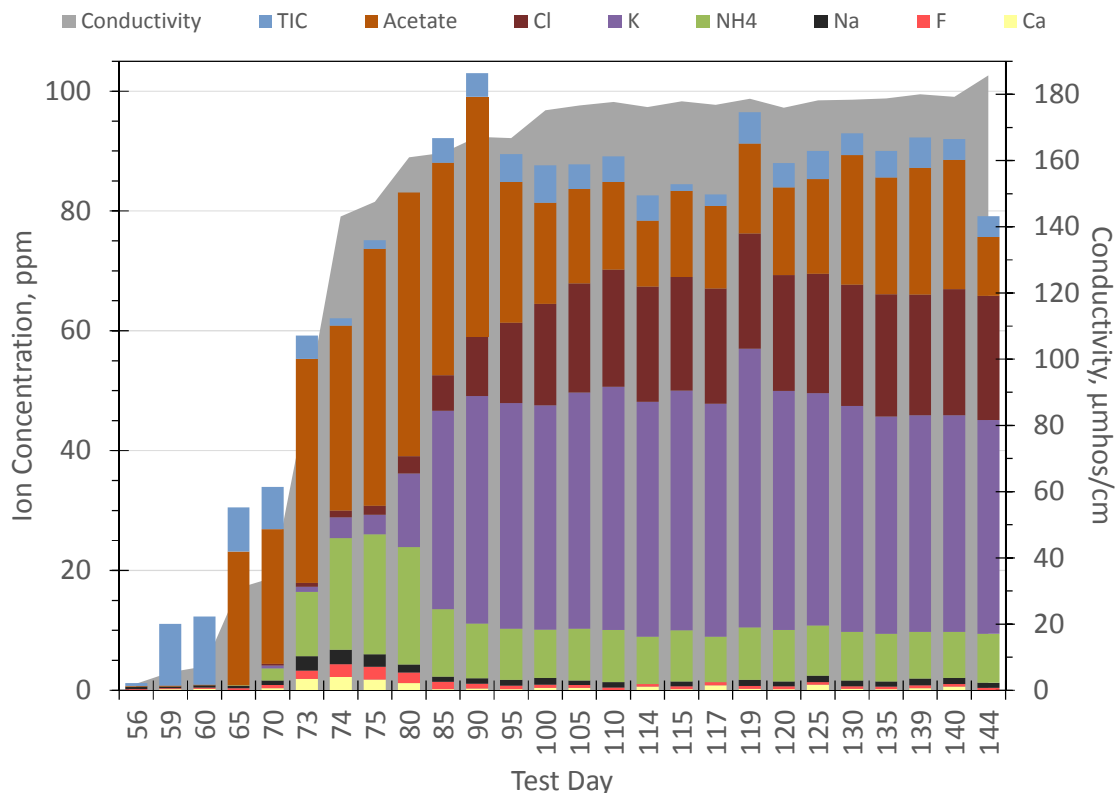


Figure 4. Bed #1 breakthrough ion characterization profile. All data are representative of aliquots sampled on the test day indicated and analyzed off-line by the MSFC ECLSS Chemistry Lab.

Figure 5 displays the MF Bed #1 total organic carbon breakthrough profile and single-pass adsorption efficiency. Single-pass adsorption efficiency was defined in accordance with Eq. 2.

$$\eta = \frac{TOC_{in} - TOC_{out}}{TOC_{in}} \times 100\% \quad (2)$$

The inlet TOC was remarkably consistent over the test lifetime averaging 55.2 ± 3.6 ppm. Overall, the trend in adsorption efficiency decreased over time, as expected for a gradual saturation of the Ambersorb activated carbon spheres. There was a noticeable dip in the adsorption efficiency beginning around Test Day 65 and continuing through Test Day 95. Overlaid with the TOC data is the Bed #1 conductivity trend data. The apparent drop in adsorption efficiency was attributed to the superposition of ion breakthrough, most notably the organic acetate ion rather than any organic desorption from the carbon itself. In summary, the Ambersorb in Bed #1 displayed an efficiency of approximately 55% at test start and this dropped to 30% at test end (17,771 lb_m Ersatz water).

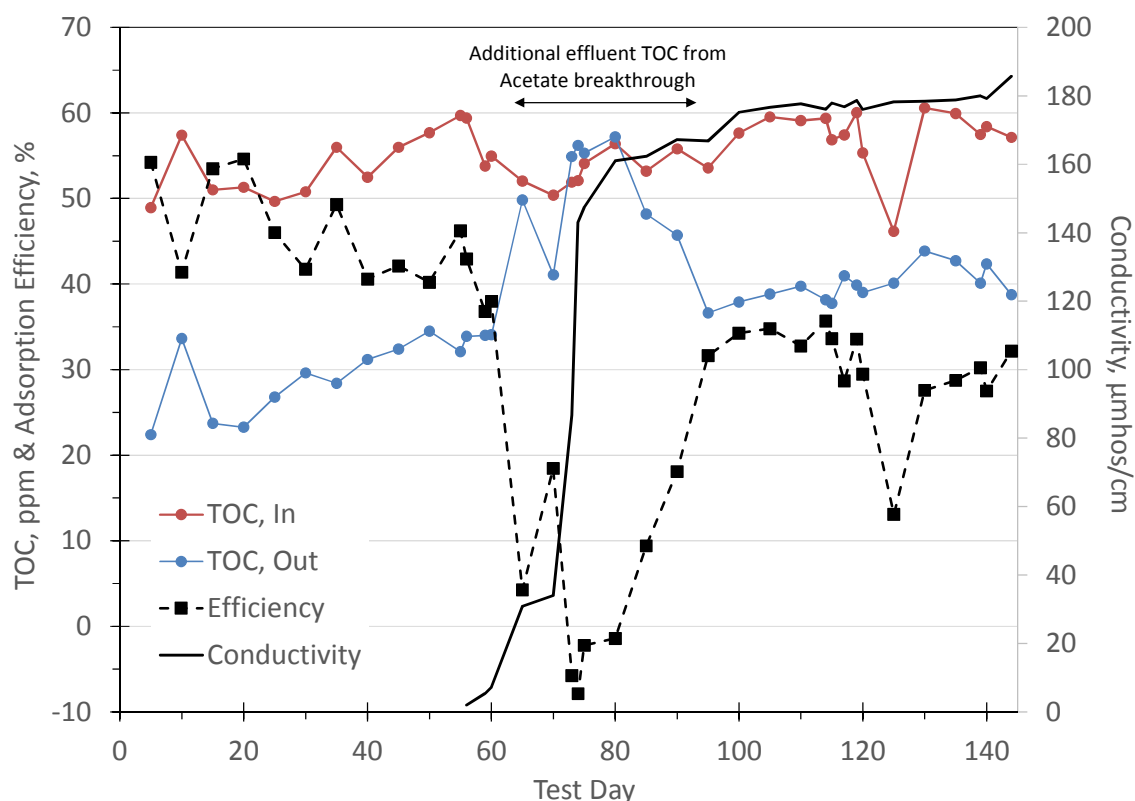


Figure 4. Bed #1 total organic carbon breakthrough profile and single-pass adsorption efficiency. All data are representative of aliquots sampled on the test day indicated and analyzed off-line by the MSFC ECLSS Chemistry Lab.

C. Bed #2 Effluent Characterization

Figure 6 displays the overlaid conductivity, ion species, and pH breakthrough correlations for Bed #2. Note that the 1st plateau of Bed #2 was so short-lived (see Fig. 2) that only one sample was collected on Day 117. In addition, lab samples measured by conductivity dip probe on days 100 through 110 were higher than believed to be if measured using a flow cell (liquid junction artifact) and should not be confused with the 1st breakthrough plateau. The bed breakthrough profile was accompanied by a decrease in process pH over the 1st and 2nd conductivity plateaus before slightly increasing upon complete ion breakthrough. Analysis of the major ionic constituents indicated the initial pH drop was first due to the breakthrough of dissolved TIC followed closely by acetate. These two contaminants emerge as the main constituents in the 1st and 2nd conductivity plateaus, respectively. The onset of the final conductivity breakthrough was delayed as compared to Bed #1. As compared to Fig. 2 and Fig. 3, the duration of the 2nd plateau was increased for Bed #2 lasting approximately 2,500 lb_m of throughput versus only 750 lb_m for Bed #1. A slight increase in ammonium was observed which appeared to slightly increase the process pH. The test program was terminated before complete ion breakthrough was completed.

The process influent to Bed #2 was not representative of the true Ersatz conductivity until at least Test Day 74 (9,083 lb_m). This puts the mass throughput until the initial breakthrough on Test Day 114 at 4,931 lb_m which is reduced as compared to Bed #1 at 6,897 lb_m. This discrepancy can be rationalized by observing that prior to Test Day 74, the breakthrough products from Bed #1 fed a low conductivity process stream into Bed #2 which included 353 lb_m at a mean load of 74 µmhos/cm (TIC, acetate & ammonium), 1,205 lb_m at 33.5 µmhos/cm (TIC and acetate), and 1,043 lb_m at 10.5 µmhos/cm (TIC). The persistent presence of TIC in the Bed #2 feed over this initial 2,600 lb_m of breakthrough prior to Test Day 74 explains the observed short lived 1st plateau. The extension of the 2nd plateau must be related to the delayed breakthrough of ammonium and is also likely related to the varied influent history of Bed #2.

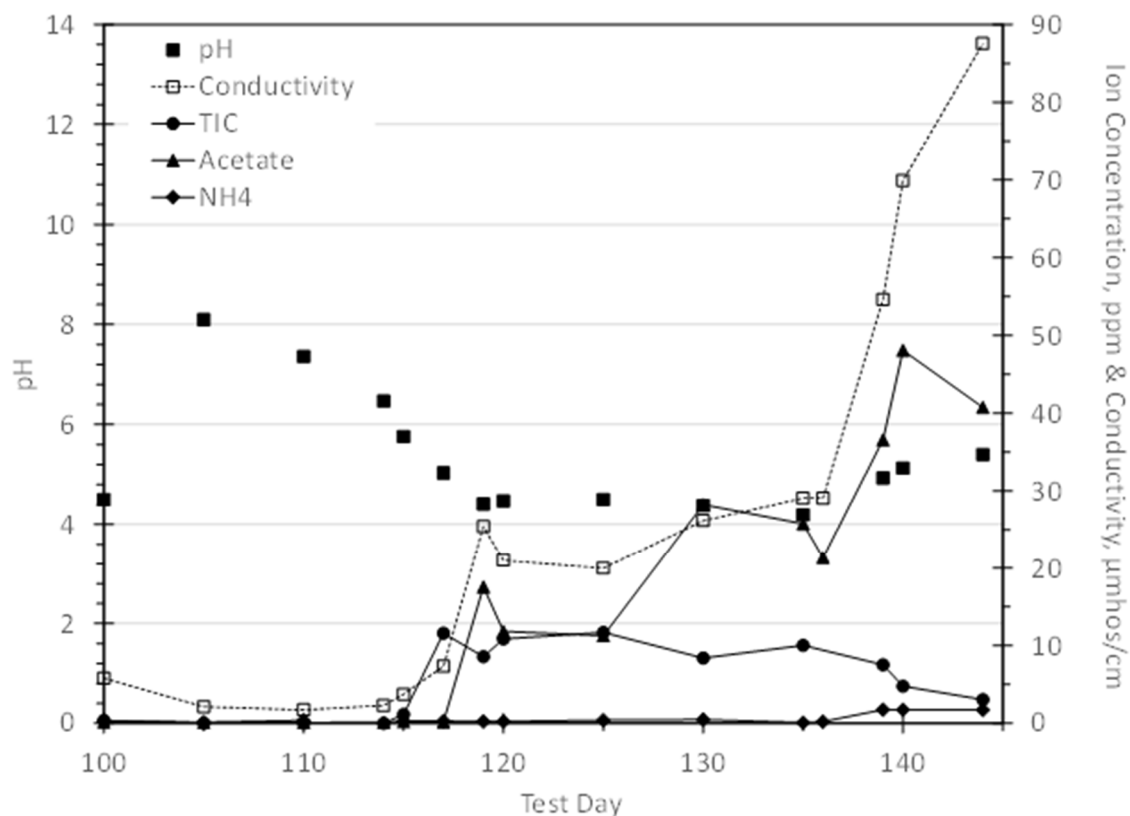


Figure 6. Bed #2 breakthrough conductivity, major ion species, and pH correlations. All data are representative of aliquots sampled on the test day indicated and analyzed off-line by the MSFC ECLSS Chemistry Lab.

Figure 7 displays the complete profile of the Bed #2 breakthrough ion species showing inorganic carbon as the 1st major breakthrough species (Day 117) followed by acetate (Day 119). Note, TIC was not analyzed in Test Day 136 and is therefore absent from Fig. 7. During the 1st conductivity plateau, calcium, sodium, and fluoride were detected at levels ≤ 0.5 ppm. Detailed analysis results are given in Table A2 and discussed further below. Additionally, trace levels of chloride were observed in the 2nd conductivity plateau. Sulfate appears near the final breakthrough. Similar to Bed #1, ammonium was the primary breakthrough product for the final conductivity rise.

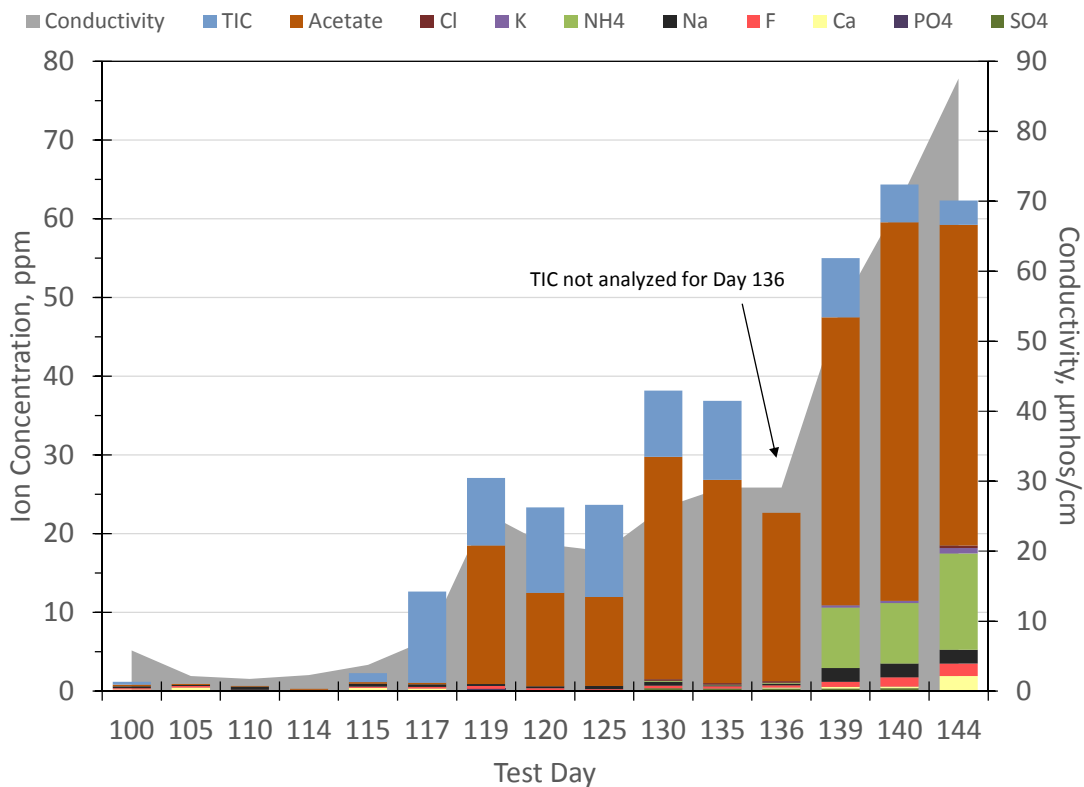


Figure 7. Bed #2 breakthrough ion species characterization profile. All data are representative of aliquots sampled on the test day indicated and analyzed off-line by the MSFC ECLSS Chemistry Lab.

Figure 8 displays the Bed #2 total organic carbon breakthrough profile and single-pass adsorption efficiency. The inlet TOC content to Bed #2 was dependent on the effluent from Bed #1 and therefore was comprised of any organic carbon not readily adsorbed in the first bed but also any upstream organic acetate breakthrough. The Bed #1 breakthrough of acetate, as described by Fig. 8, was observed in the inlet to Bed #2 around Test Day 65. This caused an artificial rise in the calculated single-pass adsorption efficiency. Similarly, breakthrough of acetate through Bed #2 caused a large drop in the efficiency starting around Test Day 125. Overall, the trend in adsorption efficiency decreased over time. The observed performance of Ambersorb in Bed #2 is handicapped by the fact that most of the readily adsorbable TOC was already removed in Bed #1 leaving only lighter, less adsorbable organics influent to Bed #2. Nevertheless the initial adsorption efficiency was approximately 20% and this dropped to 15% before the data was skewed by Bed #2 acetate breakthrough as shown by the overlaid conductivity trend data.

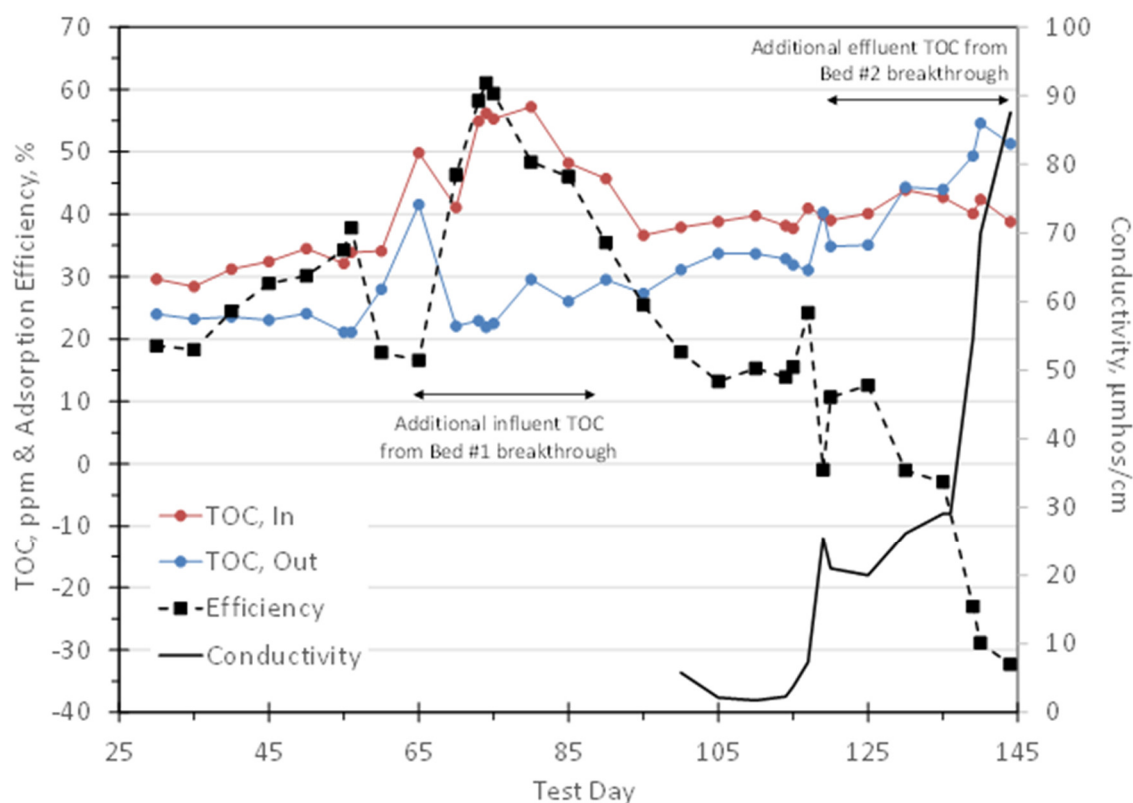


Figure 8. Bed #2 total organic carbon breakthrough profile and single-pass adsorption efficiency. All data are representative of aliquots sampled on the test day indicated and analyzed off-line by the MSFC ECLSS Chemistry Lab.

D. Multifiltration Bed Lifetime Extension Discussion

Based on the bed breakthrough characterization data presented herein, potential operational changes can be considered. Remarkably, in allowing Bed #1 to saturate and pass all breakthrough products to Bed #2 the onset of ammonium breakthrough in Bed #2 appeared to be delayed. By allowing MF Bed #1 to completely saturate and breakthrough, and also operating MF Bed #2 to Test Day 136, a total of 16,770 lb_m (7,606 L) of water can be processed by the half-scale beds before R&R. In this scenario, an inorganic load consisting of predominantly TIC and acetate (Fig. 7, Test Days 119 to 136) would be passed to the catalytic reactor. Mean residual contaminants (mg/L) over this time-period are: TIC = 9.9 ± 1.4 ; Na⁺ = 0.30 ± 0.1 ; F⁻ = 0.30 ± 0.04 ; Cl⁻ = 0.20 ± 0.01 ; C₂H₃O₂⁻ = 19.4 ± 7.1 . Ions not listed had mean values ≤ 0.1 mg/L. The TOC over this time was 39.7 ± 4.6 ppm. The bed should be pulled at first sign of the next conductivity rise due to threat of sulfates (~ 0.35 mg/L) reaching the catalyst. It therefore follows that testing be conducted with an Ersatz water load representative of these specific test days on the developmental catalytic reactor at MSFC. For conservatism, mean plus one standard deviation Ersatz loads are recommended for this evaluation. Note that this reactor contains the same quantity of flight catalyst as that employed in the ISS WPA, and was manufactured per the same process by the supplier, United Technologies Aerospace Systems (UTAS). While the reactor might have capacity for the ammonium load, the presence of many other inorganic species during the final breakthrough trend makes allowing these products to pass downstream unattractive. Should some ammonium reach the reactor it is important to consider the potential implications for the process and for the spacecraft product water and air quality.

The catalytic wet oxidation (CWO) of ammonia is of practical importance for remediation of toxic industrial wastewaters (see Ref. 9 and citations within).⁹ In specific, complete selective oxidation to form molecular nitrogen is desired. In general, CWO of ammonia requires harsh temperatures and pressures to proceed and has been characterized as very slow without a catalyst (see Ref. 10, 11 and included citations).^{10,11} Fortunately, varied catalyst

formulations have shown certain Group 8-10 elements (VIII B), such as Ruthenium, exhibit high activity.¹⁰ CWO has been achieved at temperatures and pressures comparable to the WPA and is pH sensitive.⁹ Ammonia oxidation is enhanced at high pH due to favorable reaction kinetics of ammonia over ammonium.¹⁰ This pH effect is apparent from studying the mechanism proposed by Lee et. al (2005) wherein molecular ammonia must be present to form nitrite (via intermediate nitrous acid dissociation) which in turn can then react with ammonium to molecular nitrogen.⁹ In considering any potential ECLSS impacts associated with such an operational change, there is concern that reaction intermediates, like nitrite (NO_2^-) may persist and possibly evolve nitrogen oxides (NO_x) in the vapor phase. Nitrite may only be formed, however, by a cascade of reactions in which nitrous acid is formed from dissolved molecular ammonia. As shown by Fig. 6, this is not the case for the Bed #2 effluent where the pH averaged around 4.3 near breakthrough. At room temperature, the ammonium fraction is near unity for this pH.⁸ Furthermore, if oxygen is in excess, such as in the WPA, then additional oxidation of any nitrite to nitrate (but also decreases N_2 yield) should further alleviate concerns of NO_x evolution.⁹ Finally, the reaction of nitrite with ammonium (present in excess to any ammonia) to molecular nitrogen is also kinetically favored. Therefore, the permission of ammonium to the catalytic reactor may be acceptable but testing should be carried out to characterize the reactor product dissolved/evolved species and well as effluent pH.

III. WPA Ambient Catalyst Development

In response to a competitive RFP released in April 2014 titled “ISS Water Processor Assembly Ambient Catalytic Reactor Catalyst Development,” contracts were awarded to two offerors (United Technology Aerospace Systems and Umpqua Research Company) in pursuit of development of WPA catalyst with enhanced activity capable of operation at ambient system pressures. Performance goals for effluent TOC and a required ersatz water definition were provided by NASA MSFC for benchmarking catalyst activity. As a result of these research efforts two full-scale volumes of catalyst will be delivered to MSFC for evaluation in 2016. Both catalyst formulations include VIII B group element(s) deposited on a porous support. As discussed by Ping et al. (2016), the UTAS catalyst is supported on alumina¹² whereas the UMPQUA catalyst is supported on zirconia.[¥] The two supports differ based on their bulk density, surface area, and pore/channel sizes. Alumina supports generally have one order of magnitude greater surface area than zirconia but the higher zirconia density may offset some of this effect in a fixed volume reactor. Furthermore, the reaction rate can be limited by diffusion of the reactants/products to and away from the support and this is enhanced in supports with increased pore/channel sizes. However, there is a general tradeoff between increased support surface area and decreased pore/channel size. The competing effects of each support’s physical properties will be empirically discerned by reactor performance testing.

In order to thoroughly evaluate each catalyst’s activity and stability, performance testing and long duration testing will be conducted. Testing on each developmental catalyst formulation will be carried out in parallel using the Aqueous Phase Catalytic Oxidation test stand and the Thermal Catalyst Test Stand located at MSFC. Process flowrates will be standardized (13 lb_m/h Ersatz water; 0.011 lb_m/h O_2) and two separate challenge Ersatz water formulations will be used for evaluation: 1) Standard Ersatz Formulation (alcohols, aldehydes, acetone, glycols; TOC = 35.8 mg/L) and 2) Challenge Ersatz Formulation (elevated Standard Ersatz load plus formic acid and urea; TOC = 64.8 mg/L). Each catalyst will be challenged over a range of temperatures 200°F to 270°F and at both elevated (45 psig) and ambient system backpressures. Reactor effluents will be sampled and analyzed for TIC/TOC, alcohols (including acetone), acetate, pH, and conductivity. In addition, reactor effluents will be sampled for particle size distribution analysis. Catalyst performance testing will be carried out over 18 test days. After this time each reactor will be left idle at 270°F and at 6 month intervals will be challenged with 12 days of performance testing utilizing varied temperatures and pressures for each Ersatz formulation. Testing will continue until a satisfactory test duration is achieved or until catalyst performance degradation is observed.

IV. UPA Upgrades

As of April 2, 2016, the total UPA production on ISS was 11,214 L (24,715 lb_m) of distillate from crewmember urine since initial operation in 2008. Over that time, a total Orbital Replacement Unit (ORU) mass of 4,489 lb_m (2,036 kg) has operated in the UPA, including initial hardware installation, replacements of failed ORUs, and improved hardware like the ARFTA. Overall, the UPA hardware replacement rate is currently 0.18 lb_m of hardware per 1 lb_m of distillate that has produced. In the pursuit to reduce replacement rates by improving robustness, durability, and extended life, several upgrades have been under evaluation. Once developed, these upgrades will be incorporated into ISS UPA ORUs to collect extended performance demonstration in an operational flight environment. Successful

[¥]Information provided by John Holtsnider at UMPQUA Research Company.

demonstrations will provide tangible life cycle cost benefits to the ISS over its remaining operational life and increase confidence that the UPA design can meet demanding exploration mission needs.

A. Parametric Test and Thermal Model

The development of the vapor compression distillation (VCD) technology primarily occurred at Life Systems International in the 1980's based on an empirical test effort. Though the VCD technology has operated well on ISS, the UPA engineering team believes performance can be improved by optimizing the system operation. To improve the overall understanding of the system operation, a parametric test was completed to evaluate multiple operational parameters of the VCD. These parameters include the system pressures and temperatures, motor currents, production rate, and distillate conductivity and quality. In addition to the standard pressure and temperature instrumentation, the DA was also outfitted with remote temperature sensors installed inside the evaporator and stationary bowl to provide insight into the thermal transients during VCD operation.

In parallel with this effort, the MSFC Thermal Analysis and Control Branch (EV34) has developed fluids and thermal models of the VCD using the COMSOL Multiphysics¹³ and Thermal Desktop¹⁴ modeling packages to demonstrate and predict VCD performance. The models are correlated to data from the parametric test and will ultimately be used to identify the optimal operating conditions for the VCD. In addition, the models will be used to determine if the distillation assembly (DA) size can be reduced (either length or diameter) while maintaining production rate and distillate quality. A COMSOL model of the DA evaporator volume is shown below in Figure 9.

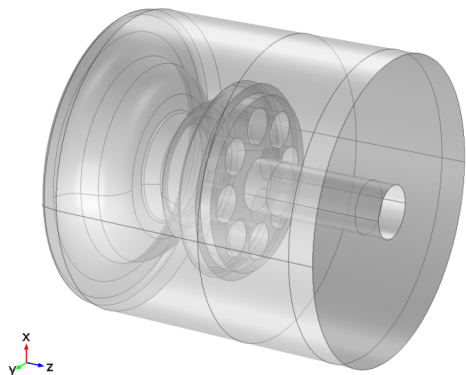














Figure 9. DA Evaporator Model in COMSOL

A summary of findings from the evaluation of parametric test data and correlation of the VCD, Pressure Control and Pump Assembly (PCPA) and Fluids Control and Pump Assembly (FCPA) models is presented in Table 2. Each potential enhancement or optimization is listed with an impact evaluation and explanation. The enhancements are parsed into three categories representing operational changes, modest hardware changes and significant hardware changes. Operational changes could presumably be implemented on existing hardware with little to no impact (and most were through the parametric test program).

Table 2. Parametric Test/Model Correlation Findings

		Impact	Comments
Operational Change	Variable Motor Speed (Compressor/Centrifuge Synchronous)		Significant improvement in production rate.
	FCPA Pump Rate Increase		Additional recycle flow may increase evaporator film thickness.
	PCPA Pump Rate Increase		Model prediction possible.
	Variable Condenser/Evaporator Pressure		P16 set point correlation TBD.
	Low Temperature Coolant		12% increase in PCPA performance.
	Stationary Bowl Heater Set Point		Significant power reduction (up to 50%)
Small/Moderate Hardware Changes	Asynchronous Compressor/Centrifuge Speed		Stackable option.
	Distillation Assembly Recuperative Heat Exchanger		Potential 5% increase in production rate.
	Eliminate Stationary Bowl Heaters		Significant power reduction (up to 180 Watts).
	PCPA Pump through Stationary Bowl Volume		TBD performance.
	PCPA Inlet Heat Exchanger		12% increase in PCPA performance. 20% when combined with low temperature coolant.
Significant Hardware Change	Distillation Assembly Size Reduction		Substantial volume reductions.

Increasing the DA motor speed for synchronous changes in compressor and centrifuge rotational speeds provided the single biggest improvement in production rate for all enhancements considered in the parametric test program. The production rate scaled nearly linearly with motor speed over the conditions tested. It is thought that the increased volume throughput with motor speed (of the essentially positive displacement compressor) is directly responsible for the improved production rates while boiling/condensation rates in the evaporator/condenser are not a limiting factor or at least kept pace with increases in the production rate. Through correlation, the VCD system model should be able to asynchronously optimize the compressor/centrifuge spin rates.

An interesting observation was a slight decrease in product rate with an increase in FCPA pumping rate (or recycle loop flow rate). It is conjectured that this is evidence of a dependency on evaporator film thickness. Increased recycle loop flow rate may increase the film thickness which may increase the boiling point due to hydrostatic influences (i.e. weight of the film under high rotational acceleration) on pressure. Conversely, decreases in the recycle loop flow rate may reduce film thickness thereby enhancing production rates slightly.

Changing the stationary bowl heater set-point from 130°F to 110°F had a significant impact on power consumption with reductions up to 50%. The unit operated without incident through the heater set-point changes but one caveat is that any accumulation of water in the stationary bowl volume was not quantified through the test.

As expected, PCPA enhancements for low temperature coolant and thermal conditioning of the purge flow from the DA condenser provided increases in pumping performance as indicated from model predictions. Increasing the PCPA pumping rate was not tested but could be predicted as well using the detailed PCPA model.

Analysis indicates that geometric resizing of the DA evaporator should be possible when accompanied by proportional changes in centrifuge speed. No disqualifying impacts or disturbance in the flow field from the boiling surface to vapor exiting through the demister were observed in the analysis for the cases studied. The most significant impact to modest changes in the evaporator diameter may be increases in centrifuge rotation to maintain production rate over the reduced boiling area.

B. FCPA and PCPA Valve Design

There are 3 valves that change fluid direction on the FCPA manifold. The old valve design included a static preload on the valve packing that was found to decay during thermal cycle environmental testing, requiring more manufacturing time. These valves would historically spend a minimum of 20 days in an iterative assembly process to incrementally achieve the desired preload. In order to reduce manufacturing time and create a more reliable preload, all newly assembled FCPAs include an improved packing preload design. The design added Belleville washers to maintain a dynamic preload on the valve packing, thereby removing the iterative nature of the test sequence and make the packing more reliable against cold flow. As of April 2016, four FCPAs have been successfully assembled with the improved valve design. Of these, SN004 has been installed on ISS with no performance issues observed.

C. FCPA and PCPA Drive Train

Over the life of UPA on ISS, FCPA operational life had been drastically reduced compared to the originally predicted lifespan and end of life failure of peristaltic tube wear-out. The majority of FCPA failures have been attributed to failures with the drive train. FCPA and PCPA designs have used the same harmonic drive train design, though they are operated at different speeds. All PCPA failures on ISS have been related to burst tubing, which is the expected failure for the peristaltic pumps. In contrast, the FPCAs were historically failing after an average of 600 operating hours on ISS, which is only approximately 4 months for a 6-crew urine load. It is unclear why the drive train issues have been seen so frequently in the FCPA, but not in the PCPA. Due to the frequent failures, the FCPA Mean Time Between Failures (MTBF) was reduced from the expected 8,760 operating hours to the historically averaged 600 operating hours.

To increase FCPA life and reliability, a new drive train was implemented and tested at MSFC. This new design is the planetary gear drive train, which requires less precision during assembly and operation to maintain functionality. Though the harmonic drive is good for precision applications, the planetary gear is more advantageous for power transfer situations such as the UPA peristaltic pumps. The new design was first evaluated in the FCPA used in the UPA development test bed for 2,400 hours, which is four times the MTBF established for the FCPA on ISS. The first FCPA implementing the planetary gear design was installed on ISS in October 2016 with FCPA SN004. As of March 30, 2016, FCPA SN004 has operated for 593 hours with nominal performance and lower current drawn than the previous design. Unfortunately, the ground unit failed after 3,223 hours of operation and 657 on/off cycles. The failure investigation is ongoing, but at this time it is not expected that the planetary gear design is the root cause.

D. DA O-ring Belt

Rotation of the DA is currently driven by an O-ring belt (Figure 10). However, there is an ongoing risk of the belt slipping during operation due to the steam environment in the DA. The risk is greatest at the beginning of a process run, since the steam has time to condense as the DA cools between processing. Belt slippage at startup has been consistently observed in UPA operations on ISS. In February 2016, DA SN002 experienced a failure when the belt slipped during a process cycle, causing the centrifuge speed to fall. Attempts to recover the DA operation were unsuccessful at achieving more than 30 minutes of operation. As a result, the DA SN002 was replaced at only 30% of expected life.

The failed unit will return to MSFC in the summer of 2016 for evaluation of the hardware. However, this belt was already on the list of upgrades to the system. Before the belt slip failure, the UPA had shown indications of water in the stationary bowl, which is known to happen during nominal UPA operation. The heaters around the stationary bowl volume were added to the design to evaporate the water back into the condenser and prevent it from accumulating in the stationary bowl. However, as the condensate forms in the stationary bowl, droplets may form and reach the o-ring drive belt. Ground tests have shown that only a drop of water is required to cause the belt to slip.

To improve the drive belt reliability in this environment, two design options are under consideration. A belt with teeth (such as a Gates belt design) would provide a more robust design, but would also require improved timing to insure the teeth properly interface with both pulleys. This will be challenging since the pulleys have different diameters. Another more achievable design solution is with a v-type belt. This design change was also previously evaluated, resulting in the conclusion that a tensioner would be required to insure proper function. At the time, this approach was not considered viable due to the limited space available for the tensioner location. Incorporation of this technology would drive an enlargement of the DA, which was considered an unacceptable option. With the new information gleaned from the parametric testing regarding DA resizing, both of these design options are now under consideration.

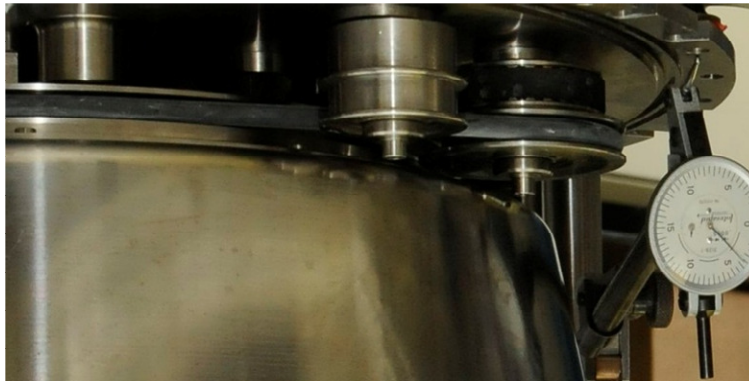


Figure 10. DA O-ring Belt

V. Conclusion

Though the initial operation of the WPA and UPA on ISS has been acceptable, improvements are highly desirable to optimize their performance on ISS and position them for use on future missions. The WPA improvements focus on reducing the resupply penalty for the WPA MF Beds and improving system reliability through the use of an improved catalyst that can operate at ambient pressure. UPA improvements are solely focused on improving system reliability by addressing known design issues currently identified from operation on ISS and manufacturing processes. Successful implementation of these upgrades will position the WPA and UPA technologies for optimum performance on ISS and execution in future manned mission beyond ISS.

Appendix

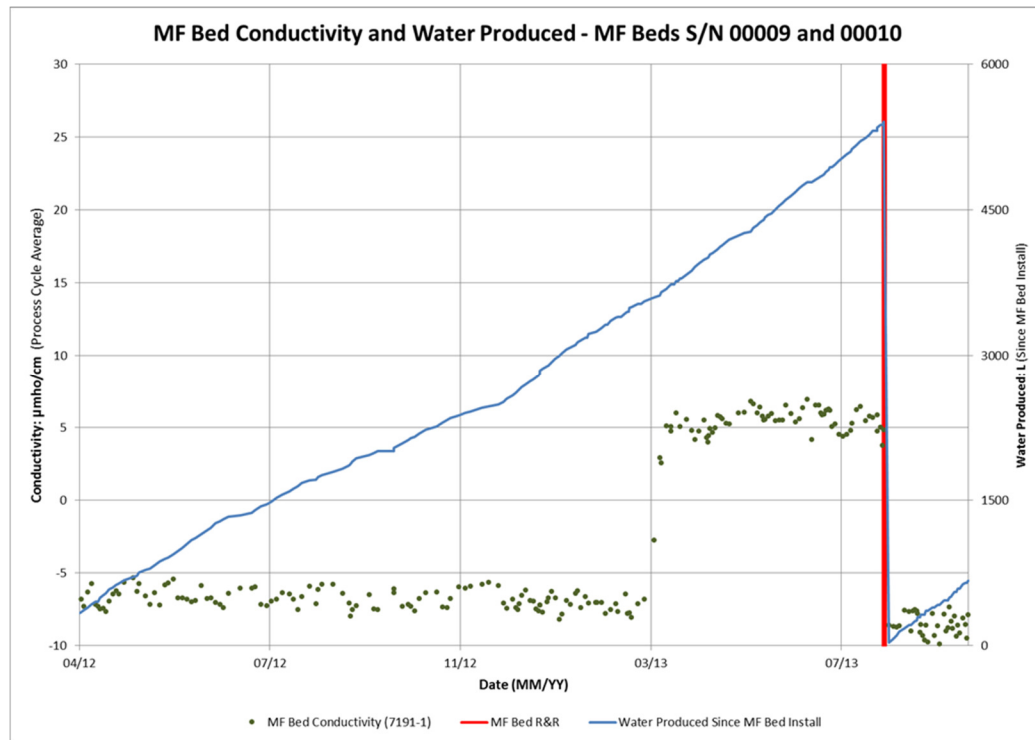


Figure A1. Flight MF Bed Data showing process conductivity and throughput.

Table A1. MF Bed #1 Lab Data Summary

Test Day	pH	COND	TIC	TOC	TOC QC	Cations [mg/L]				Anions [mg/L]				
-	-	[µmho/cm]	[mg/L]	[mg/L]	[mg/L]	Na ⁺	NH ₄ ⁺	K ⁺	Ca ²⁺	F ⁻	Cl ⁻	SO ₄ ²⁻	PO ₄ ³⁻	C ₂ H ₃ O ₂ ⁻
5			0.27	22.4	48.93									
10			0	33.64	57.4									
15			0	23.72	51									
20			0.12	23.28	51.3									
25			0	26.8	49.65									
30				29.6	50.8									
35				28.4	56									
40			0	31.19	52.5									
45	9.47		0	32.4	55.98									
50	9.46		0.004	34.5	57.7									
55			0	32.1	59.7									
56	6.72	2.01	0.51	33.9	59.4	0.4				0.19				< 0.1
59	5.1	5.45	10.3	34	53.8	0.27			0.2	0.18				0.13
60	4.82	7.22	11.41	34.08	54.94	0.37			0.28	0.18				< 0.1
65	4.27	30.84	7.39	49.82	52.04	0.4	< 0.1			0.34				22.3
70	4.65	34.0	7.03	41.08	50.38	0.78	2.0	0.44	0.38	0.5	0.3			22.5
73	5.37	86.75	3.9	54.9	51.9	2.4	10.7	0.9	1.9	1.4	0.6			37.4
74	6.43	143.1	1.25	56.2	52.1	2.4	18.6	3.5	2.2	2.16	1.1			30.9
75	6.74	147.5	1.43	55.3	54.1	2.1	20	3.3	1.8	2.1	1.5			42.9
80	7.1	161.0	0	57.2	56.4	1.3	19.6	12.3	1.2	1.78	2.9			44.0
85	7.35	162.3	4.1	48.2	53.2	0.86	11.3	33.1	0.2	1.2	5.9			35.5
90	7.51	167.2	3.99	45.7	55.79	0.93	9.1	38	0.29	0.78	9.95			40.0
95	7.53	166.8	4.66	36.63	53.58	1.0	8.5	37.7	0.2	0.56	13.39			23.5
100	7.6	175.2	6.27	37.9	57.64	1.14	8.1	37.4	0.4	0.5	16.94			16.87
105	7.55	176.6	4.09	38.82	59.53	0.78	8.66	39.4	0.4	0.47	18.22	0.35	0.28	15.75
110	7.47	177.7	4.29	39.75	59.12	0.89	8.7	40.6		0.46	19.55	0.35	0.35	14.63
114	7.95	176.1	4.26	38.17	59.36		7.89	39.22	0.65	0.4	19.22			10.97
115	7.83	177.9	1.15	37.74	56.86	0.82	8.52	40	0.17	0.5	19.0			14.33
117	7.77	176.8	1.91	40.95	57.42		7.6	38.9	0.85	0.5	19.2			13.8
119	7.93	178.7	5.21	39.89	60.03	1.0	8.75	46.5	0.27	0.48	19.23			15.05
120	7.84	176.0	4.08	39.02	55.32	0.8	8.6	39.9	0.2	0.47	19.33			14.62
125	7.8	178.2	4.68	40.11	46.15	1.08	8.38	38.74	0.89	0.47	19.97			15.8
130	8.03	178.4	3.68	43.87	60.57	0.99	8.08	37.7	0.22	0.45	20.25	0.33		21.62
135	7.82	178.8	4.47	42.72	59.94	0.82	7.94	36.28	0.19	0.46	20.4	0.34		19.5
139	7.89	180.0	5.06	40.1	57.48	1.14	7.75	36.2	0.37	0.46	20.1	0.33		21.18
140	7.78	179.2	3.48	42.34	58.4	1.0	7.7	36.18	0.6	0.44	21.0	0.32		21.6
144	7.64	185.7	3.5	38.76	57.14	0.88	8.13	35.69		0.4	20.75			9.8

Table A2. MF Bed #2 Lab Data Summary

Test Day	pH	COND	TIC	TOC	TOC Bed #1	Cations [mg/L]				Anions [mg/L]				
-	-	[μmho/cm]	[mg/L]	[mg/L]	[mg/L]	Na ⁺	NH ₄ ⁺	K ⁺	Ca ²⁺	F ⁻	Cl ⁻	SO ₄ ²⁻	PO ₄ ³⁻	C ₂ H ₃ O ₂ ⁻
30				24.0	29.6									
35				23.2	28.4									
40			0	23.56	31.19									
45			0	23.04	32.4									
50			0.04	24.1	34.5									
55			0.36	21.1	32.1									
56			0.36	21.09	33.9									
60			0.2	28.0	34.08									
65			0.09	41.54	49.82									
70			0	22.06	41.08									
73			0	22.96	54.9									
74			0	21.9	56.2									
75			0.04	22.5	55.3									
80			0	29.53	57.2									
85			0.43	26.02	48.2									
90			0	29.5	45.7									
95			0	27.3	36.63									
100	4.5	5.8	0.37	31.1	37.9	0.24			0.2	0.18				0.19
105	8.1	2.14	0	33.69	38.82	0.13			0.47	0.19				< 0.1
110	7.36	1.74	0	33.67	39.75	0.38				0.18				< 0.1
114	6.47	2.29	0	32.86	38.17					0.18				0.13
115	5.76	3.76	1.15	31.89	37.74	0.32			0.4	0.2				0.22
117	5.03	7.34	11.6	31.03	40.95	0.31			0.34	0.2				0.2
119	4.41	25.45	8.59	40.27	39.89	0.25				0.37			0.28	17.57
120	4.47	21.01	10.87	34.85	39.02	0.25			< 0.1	0.27				11.85
125	4.5	20.0	11.7	35.06	40.11	0.4				0.26				11.3
130	4.38	26.2	8.41	44.33	43.87	0.49	< 0.1			0.34	0.2	0.36		28.28
135	4.19	29.09	10.05	43.96	42.72	0.1	< 0.1			0.28	0.21	0.34		25.8
136		29.09				0.21	< 0.1		0.14	0.28	0.2	0.32		21.4
139	4.93	54.66	7.54	49.33	40.1	1.75	7.68	0.28	0.2	0.63		0.34		36.6
140	5.13	69.94	4.79	54.56	42.34	1.75	7.68	0.28	0.2	1.2		0.35		48.11
144	5.4	87.54	3.05	51.29	38.76	1.74	12.24	0.7	1.9	1.6	0.3			40.77

Acknowledgments

The authors would like to acknowledge the design and test engineers at MSFC that are developing and evaluating the hardware upgrades addressed in this paper.

References

- ¹Pruitt, J.M., Carter, D.L., Bagdigian, R.M., and Kayatin, M.J., "Upgrades to the ISS Water Recovery System," ICES 2015-133, *45th International Conference on Environmental Systems*, Bellevue, Washington, 2015.
- ²Carter, D.L., Pruitt, J.M., Brown, C.A., Schaezler, R.N., and Bankers, L.A., "Status of ISS Water Management and Recovery," ICES 2015-073, *45th International Conference on Environmental Systems*, Bellevue, Washington, 2015.
- ³Carter, D.L., Bowman, E.M., Wilson, M.E., Gentry, G.J., and Rector, T.J., "Investigation of DMSD trend in the ISS Water Processor Assembly," AIAA 2013-3510, *AIAA 43rd International Conference on Environmental Systems*, Vail, Colorado, 2013.
- ⁴Carter, D.L., Perry, J.L., Kayatin, M.J., Wilson, M.E., Gentry, G.J., Bowman, E.M., Monje, O.A., Rector, T.J., and Steele, J.W., "Process Development for Removal of Siloxanes from ISS Atmosphere," ICES 2015-074, *45th International Conference on Environmental Systems*, Bellevue, Washington, 2015.
- ⁵Carter, D.L., Kayatin, M.J., Wilson, M.E., Perry, J.L., Rector, T.J., Agui, J.H., Gentry, G.J., Bowman, E.M., and Greene, R.D., "Design and Delivery of Filter for Removal of Siloxanes from ISS Atmosphere," ICES 2016-015, *46th International Conference on Environmental Systems*, Vienna, Austria, 2016.
- ⁶Rector, T.J., Metselaar, C., Peyton, B.M., Steele, J.W., Michalek W., Bowman, E.M., Wilson, M.E., Gazda, D.B., and Carter, D.L., "An Evaluation of Technology to Remove Problematic Organic Compounds from the International Space Station Potable Water," ICES 2014-135, *44th International Conference on Environmental Systems*, Tucson, Arizona, 2014.
- ⁷D. L. Carter, "WRS-TPS-13-106," Marshall Space Flight Center, 2013.
- ⁸Perry, J.L., and Kayatin, M.J., "The Fate of Trace Contaminants in a Crewed Spacecraft Cabin Environment," ICES 2016-091, *46th International Conference on Environmental Systems*, Vienna, Austria, 2016.
- ⁹Lee, D.K., Cho J.S., and Yoon, W.L., "Catalytic wet oxidation of ammonia: Why is N₂ formed preferentially against NO₃⁻?" *Chemosphere*, Vol. 61, No. 4, 2005, pp. 573-578.
- ¹⁰Qin, J., and Aika, K., "Catalytic wet air oxidation of ammonia over alumina supported metals." *Applied Catalysis B: Environmental*, Vol. 16, No. 3, 1998, pp. 261-268.
- ¹¹Zhang, Q., and Chuang, K.T., "Kinetics of wet oxidation of black liquor over a Pt-Pd-Ce/alumina catalyst." *Applied Catalysis B: Environmental*, Vol. 17, No. 4, 1998, pp. 321-332.
- ¹²Yu, P., Nalette, T., and Kayatin, M.J., "Development of Advanced ISS-WPA Catalysts for Organic Oxidation at Reduced Pressure and Temperature," ICES 2016-218, *46th International Conference on Environmental Systems*, Vienna, Austria, 2016.
- ¹³COMSOL (Common Solution) Multi-Physics, www.comsol.com
- ¹⁴Thermal Desktop, Cullimore and Ring Technologies, www.crtech.com